



## Influence of thermal oxidation on as-synthesized detonation nanodiamond

Xiangyang Xu<sup>a,c,\*</sup>, Zhiming Yu<sup>b</sup>

<sup>a</sup> School of Minerals Processing and Bioengineering, Central South University, Changsha 410083, China

<sup>b</sup> School of Materials Science and Engineering, Central South University, Changsha 410083, China

<sup>c</sup> Changsha Research Institute of Mining and Metallurgy, Changsha 410012, China

### ARTICLE INFO

#### Article history:

Received 27 August 2010

Received in revised form 7 March 2011

Accepted 23 March 2011

#### Keywords:

Thermal oxidation

Diamond

Nanoparticle

Surface property

Hydrophilicity

### ABSTRACT

The thermal property of an as-synthesized black powder, a detonation nanodiamond (DND) product, was first analyzed, followed by thermal oxidation to modify its surface. During the thermal treatment, the non-diamond carbonaceous shell of the black powder was oxidized, with the likelihood of forming a C–O–C bonding between carbon atoms on the particle surface. This new structure may rupture with intensified oxidation through increasing the heating temperature and prolonging the process duration. As more oxygen-containing functional groups form on the particle surface, the particle surface becomes negatively charged, and the powder turns to be more hydrophilic.

© 2011 Chinese Society of Particuology and Institute of Process Engineering, Chinese Academy of Sciences. Published by Elsevier B.V. All rights reserved.

### 1. Introduction

Using high explosives, e.g. TNT (trinitrotoluene) and RDX (cyclotrimethylenetrinitramine), as the carbon source and high pressure wave generators, nanodiamond particles can be prepared using the detonation technique (Danilenko, 2004; Dolmatov, Veretennikova, Marchukov, & Sushchev, 2004; Mironova, Petrov, & Koretz, 2003; Sakovich, Komarov, & Petrov, 2002; Staver, Lyamkin, Gubareva, & Petrov, 1984). Such detonation product (detonation soot), collected from the reaction chamber, is generally purified with hydrochloric acid to remove metal impurities, and a black powder, referred in this paper as DND-b (detonation nanodiamond-black powder) can thereupon be prepared (Dolmatov, 2001; Gubarevich, Kostyukova, Sataeva, & Fomnina, 1991). It is reported that DND-b possesses a shell–core structure, namely, the crystallite is composed of a core of cubic diamond and a shell of graphite and amorphous carbon, together with some islets of metal and metal oxides in the amorphous carbon (Aleksenskii, Baidakova, Vul', & Siklitskii, 1999). Chemical approaches such as acidic oxidation (Aleksenskii, Yagovkina, & Vul', 2004; Kulakova, 2004; Kuznetsov et al., 1991; Lyamkin et al., 1988) have been used to purify DND-b to remove the non-diamond phases. After oxidation, a gray powder (DND-g, detonation nanodiamond-gray powder) with a mean diameter of diamond crystallites of 4–5 nm

can be obtained (Krüger et al., 2005; Shenderova, Zhirnov, & Brenner, 2002).

Thermal treatment in an inert environment has been used for surface graphitization of detonation nanodiamond (Butenko et al., 2000). Some novel approaches have been designed for DND purification and surface functionalization, e.g. high-temperature treatment in hydrogen (H<sub>2</sub>, NH<sub>3</sub>) and chlorine-containing gaseous environment (Cl<sub>2</sub>, CCl<sub>4</sub>) (Spitsyn et al., 2006), while surface oxidation effect has as well been investigated (Cataldo & Koscheev, 2003). An increase of nanodiamond crystal size was observed after the powder was selectively oxidized at 430 °C in a closed tube furnace in static air at atmospheric pressure (Kuznetsov, Chuvilin, Butenko, Mal'kov, & Titov, 1994).

C–O–C bonding may take place between adjacent crystallites and primary particles, which may be one of the main mechanisms for the formation of hard aggregates (Dolmatov, 2001; Xu & Xue, 2007). The oxidation approach might be used to destroy the C–O–C bonding, aimed at restricting hard aggregate. According to a surface thermal treatment technique proposed by Xu and Xue (2007), DND-g was heated at 1273.15 K in an N<sub>2</sub> environment for surface graphitization, followed by oxidizing the sample at 723 K. Using this method the dispersion property of the powder in aqueous medium can be considerably improved. Oxidation of commercial DND products in air at 350–450 °C was found to achieve high sedimentation stability of DND hydrosols (Shenderova et al., 2006). Thermogravimetric analysis and in situ Raman spectroscopy revealed a narrow temperature range of 400–430 °C in which the oxidation of sp<sup>2</sup>-bonded carbon could occur with no or minimal loss of diamond, and the sp<sup>3</sup>/sp<sup>2</sup> ratio could be increased by up

\* Corresponding author at: School of Minerals Processing and Bioengineering, Central South University, Changsha 410083, China.

E-mail address: [xiangyang.xu@sohu.com](mailto:xiangyang.xu@sohu.com) (X. Xu).

to 2 orders of magnitude after the oxidation, thus preparing high purity 5-nm nanodiamond particles covered by oxygen-containing surface functional groups (Osswald, Yushin, Mochalin, Kucheyev, & Gogotsi, 2006).

Since surface functional groups vary with oxidation parameters, the intensity and composition of the surface groups could be adjusted with surface oxidation measures, thus modifying the behavior of particles in solution, for example, in our previous approach to treat DND-g to become more hydrophilic thus improving the dispersion of the sample (Xu, Yu, Zhu, & Wang, 2005).

As a result of the analysis of the oxidation process, a direct thermal treatment was introduced to treat DND-b within a selected temperature range of surface oxidation. The variation of surface functional groups and the corresponding influence on particle properties were thus investigated.

## 2. Experimental

DND-b powder in this study was purchased from Jinshi Nano-material Co., Gansu, China. This black sample is an unoxidized detonation product from a mixture of TNT and RDX with a mass ratio of 1:1, while water was used as the protecting medium. Muffle furnace SX2-5-11 with a rated power of 5000 W and a rated temperature of 1373.15 K was used for thermal oxidation treatment, and the ramp rate was adjusted as 10 K/min. DND-b sample (0.5 g) was heated in the furnace in a 100 mL crucible to some set temperature and after standing for some time was cooled down. Thereafter, FTIR, XRD and XPS analyses were carried out, while the surface electronic property and particle dispersion behavior were investigated. For each condition, several samples were treated to obtain enough powder for further analysis and dispersion tests.

Using a thermal analysis system SDT 2960 (TA Instruments, USA), differential thermal analysis and thermal gravimetric analysis (DTA–TGA) were carried out in ambient air. The sample was heated from room temperature to 1273.15 K at a ramp rate of 10 K/min. The crystal structure of samples was studied using a diffractometer D/max-rA (Rigaku, Japan) with Cu K $\alpha$  as the X-ray ( $\lambda = 0.15418$  nm) radiation source.

FTIR was used for surface functional group analysis. Absorption intensity data were recorded in the spectral range 4000–400  $\text{cm}^{-1}$  using Nexus 470 (Thermo Nicolet, USA), and the samples were prepared using the standard technique of KBr-pellet. X-ray photoelectron spectroscopy (XPS) was used for analysis of chemical composition and binding status of surface elements. Measurements were performed on a VG-Escalab 220i spectrometer (VG Company, UK) with Al K $\alpha$  radiation (1486.7 eV) as X-ray excitation source and with constant analyzer energy of 40 eV and power of 300 W, and with analysis chamber vacuum of  $3 \times 10^{-9}$  mbar.

Zetasizer3000HS (Malvern Inc., UK) was adopted for photon correlation spectroscopy (PCS) analysis on particle size distribution (PSD) and surface zeta ( $\zeta$ ) potential. He–Ne radiation source ( $\lambda = 633$  nm) was used and the angle of incident was fixed as  $90^\circ$ . The pH value of the aqueous medium was adjusted with hydrochloric acid and sodium hydroxide.

## 3. Results and discussion

### 3.1. Thermal property of original DND-b

Result of DTA–TG analysis of DND-b are shown in Fig. 1. The weight loss of the sample can be roughly classified as three stages:

- **Dewatering stage.** Along with increasing surrounding temperature, the adsorbed water was removed at temperature ranging

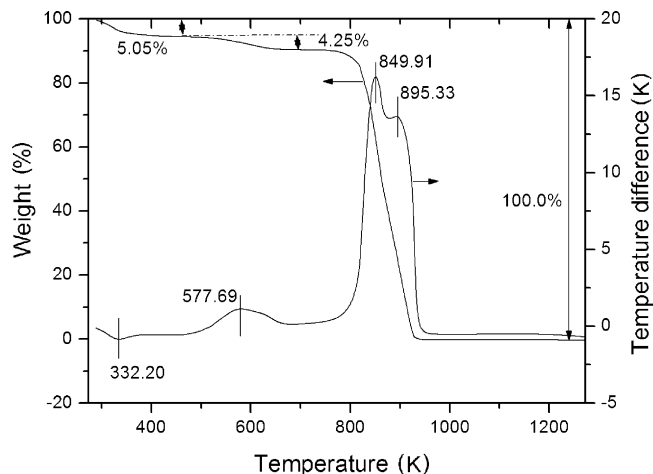


Fig. 1. DTA–TGA thermogram of original DND-b powder.

from 300 K to a little over 373 K, and at 400 K, the weight loss amounts to 5.05%.

- **Surface oxidation stage.** After removal of adsorbed water, weight loss continues, amounting to 4.25% in the range of 500–700 K. This weight loss is seen as a weak exothermic peak centered at 577.69 K, which may be attributed to decomposition of surface functional groups of DND-b.
- **Bulk oxidation stage.** A fast and drastic loss in weight started when the temperature reached an initial bulk oxidation temperature (around 800 K). This process lasts until a temperature range of 900–950 K, during which, almost all the carbonous materials in DND-b, including diamond, graphite and amorphous carbon, are oxidized. Two exothermic peaks located at 849.91 and 895.33 K were observed, which may correspond to the oxidation

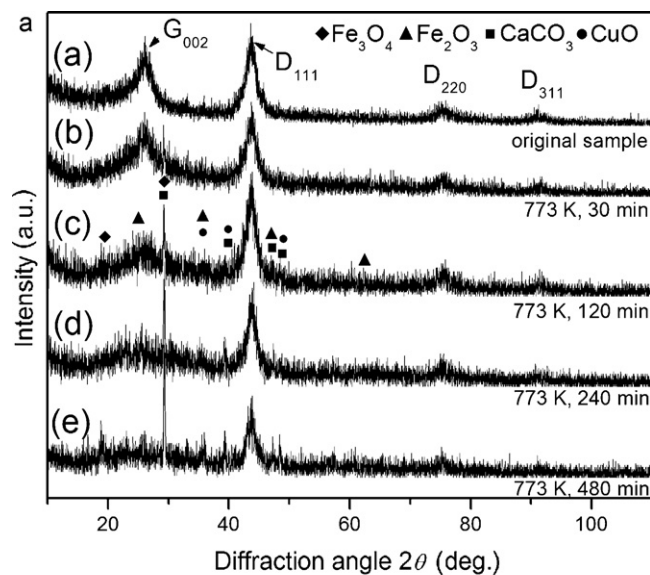


Fig. 2. XRD patterns for DND-b during thermal treatment (top) and visual observation of DND-b heated at 773 K (bottom).

of graphite and diamond, respectively. After the thermal treatment process, the powder was totally oxidized while the weight loss reached 100%.

According to the above thermal analysis, to achieve surface oxidation while avoiding drastic loss in powder weight, namely bulk oxidation, the highest heating temperature was set to be 773 K, a little lower than the initial bulk oxidation temperature, and higher than the decomposition temperature of 577.69 K.

### 3.2. Transformation of crystal structure

Transitions of crystal structure can be observed from XRD patterns of DND-b amid the thermal treatment process, as shown in

Fig. 2. For original sample and the sample heated at 773 K for 30 min, a strong diffuse diffraction peak can be observed at  $2\theta$  angle of  $26^\circ$ , showing that, when heated at 773 K for 30 min, the oxidation of graphite and amorphous carbon in DND-b was quite limited, whereas with prolonging heating duration from 30 to 480 min, intensity of the diffuse diffraction peak was gradually weakened, and even disappearing after 480 min of thermal treatment, while the main characteristic patterns are of cubic diamond structure. Meanwhile, some carbonate, oxide and even metal, such as  $\text{CaCO}_3$ ,  $\text{CuO}$  and  $\text{Fe}_2\text{O}_3$ , appeared, and, according to calculation using the Scherrer formula, the crystallite of such impurities is quite small, indicating that, there is some sub-nano carboxide, oxide and metal in DND-b, species surrounded by amorphous carbon shell before

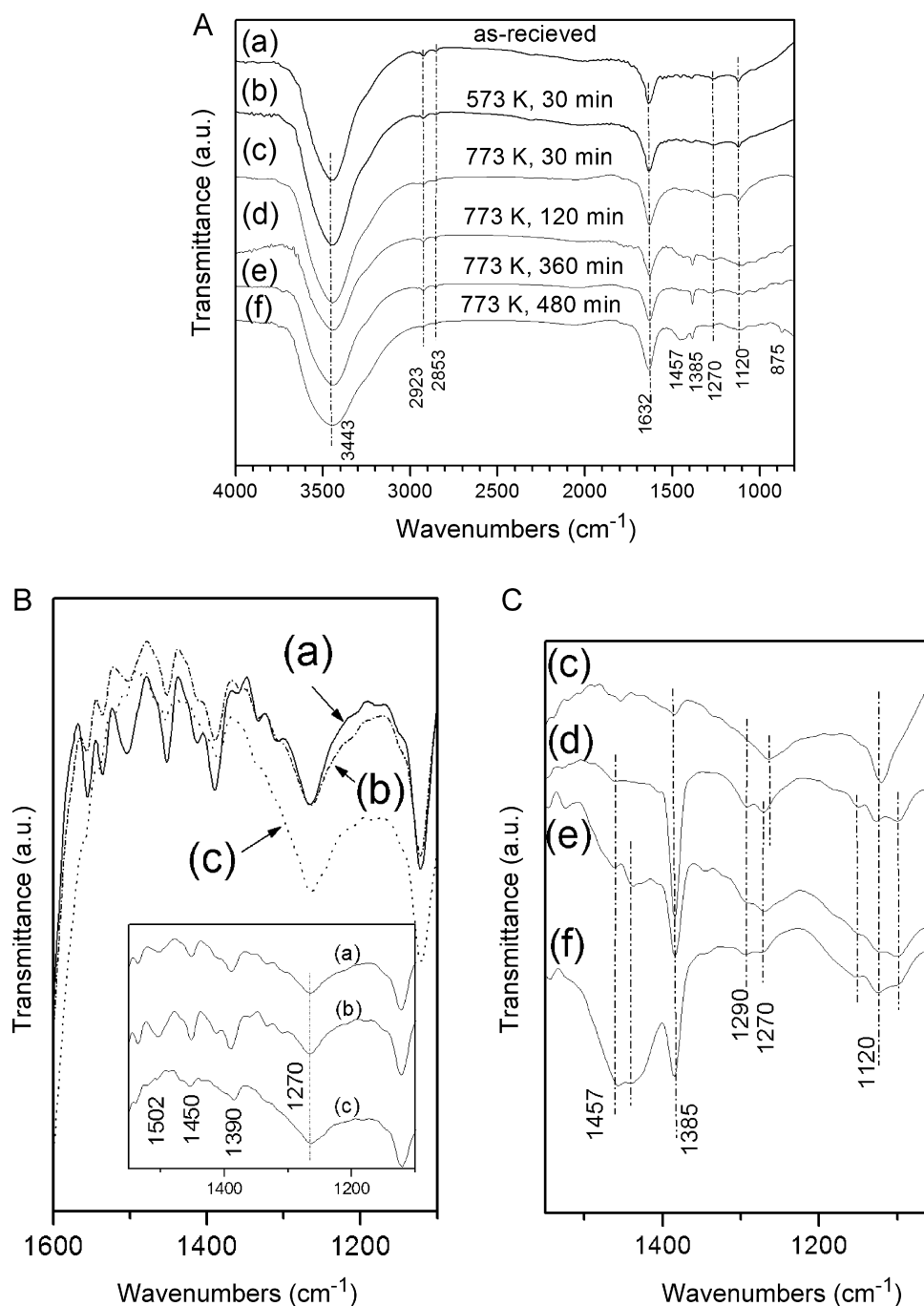


Fig. 3. FTIR spectra of DND-b during the thermal treatment.

thermal treatment, and with the oxidation and removal of amorphous carbon and graphite, the diffraction peaks of impurities appeared and the crystal structure can even be more distinguishable.

The appearance of the powder shows that, after heat treatment at 773 K for 30 min, the powder is still black, indicating that the oxidation of graphite shell is not complete, and, with prolonging duration of thermal treatment, the color turns to be increasingly lighter. After heat treatment for 120, 240, 360 and 480 min (Fig. 2, bottom), the color of the sample turns to dark gray, gray, light gray and earth yellow, respectively, indicating that the shell structure may have been oxidized thus exposing the inner core of diamond.

### 3.3. Alteration of surface properties

#### 3.3.1. FTIR spectra

Compared to the original powder, the sample heated at 573 K shows no change in FTIR spectra, as their curves are almost superposable (Fig. 3(A) and (B)). When treated at 773 K, intensity of the absorption peak at  $1270\text{ cm}^{-1}$  was first strengthened (Fig. 3(B)), which may be attributed to C–O–C stretching vibration, indicating that a C–O–C bonding had formed during the heating process. Yet, when the heating process was further prolonged, this peak would

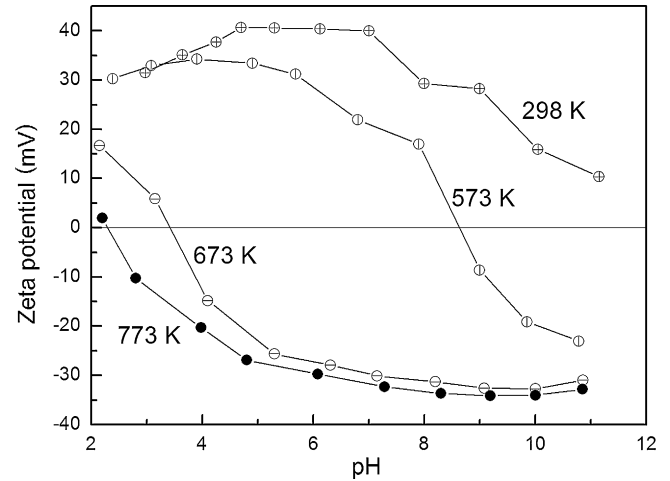


Fig. 4.  $\zeta$ -pH curves of original DND-b (298 K) and DND-b samples after thermal treatment at 573 K, 673 K and 773 K for 30 min.

again be weakened (Fig. 3(C)), showing that the C–O–C bonding was again ruptured with intensified oxidation.

Absorption bands near  $1457\text{ cm}^{-1}$  and  $875\text{ cm}^{-1}$ , which may correspond to the absorption of inorganic ions such as  $\text{CO}_3^{2-}$ ,

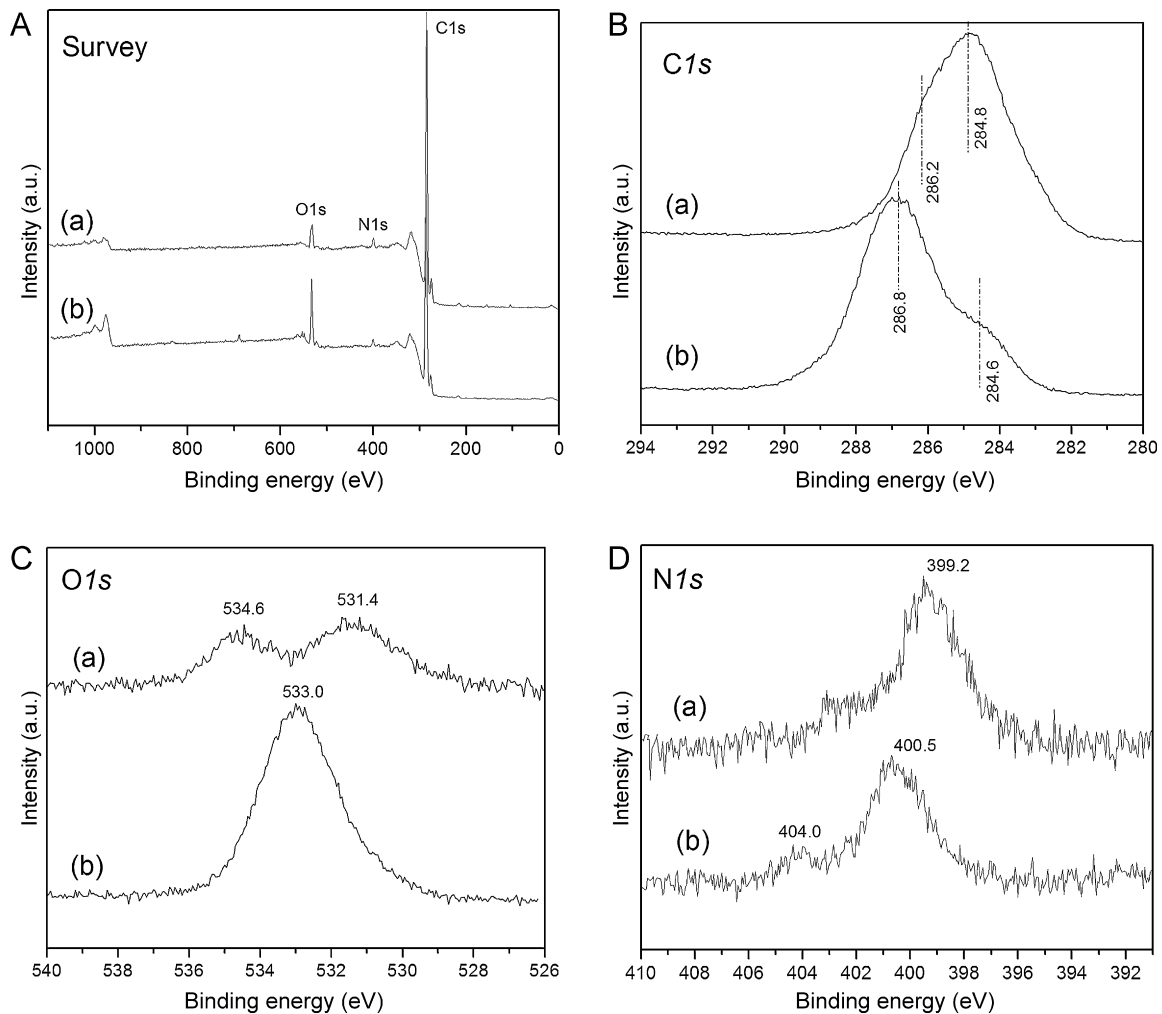


Fig. 5. XPS spectra of (a) original DND-b and (b) sample heated at 773 K for 30 min. (A) Wide-scan survey spectra for all elements, and (B)–(D) are high-resolution spectra respectively for C(1s), O(1s) and N(1s) signals.

**Table 1**

Atom percentage of main elements (C, O and N) on DND-b before and after thermal treatment.

Element	Atom percentage	
	Original sample	Heated at 773 K for 30 min
C	92.826	88.845
O	3.966	9.156
N	2.244	1.589

appeared and became strengthened with prolonged thermal treatment, showing that the ambient oxygen may react with the carbon atoms, metal and metal oxide on DND-b to form the carbonate structure. The signal at  $1385\text{ cm}^{-1}$  was intensified after heat treatment at 773 K from 30 to 480 min, possibly due to the increase of nitro groups.

### 3.3.2. $\zeta$ -Potential of DND-b in aqueous medium

Before thermal treatment (at 298 K), the original DND-b is shown in Fig. 4 to be positively charged throughout the whole pH range. This phenomenon may be attributed to the composition of surface species. As there are some metals or metal oxides on DND-b surface, hydrolysis of these species may yield more cations on the particle surface.

After heat treatment for 30 min at 573 K, a temperature slightly lower than the decomposition temperature of surface functional groups, the  $\zeta$ -pH curve of the sample overlaps the original curve at low pH values of 2–4. For pH range above 4, the  $\zeta$ -potential declined significantly, and when pH value is above 8.5, DND-b turns to be negatively charged, with the largest  $\zeta$ -potential difference between these two samples of over 40 mV. The change of surface electric potential is attributed to the hydrolysis of increased oxygen-containing groups on particle surface.

Further, after treatment at 673 K, even greater shift can be observed, that is, the  $\zeta$ -potential is further markedly reduced, with the largest  $\zeta$ -potential difference between this sample and the original one amounting to be over 70 mV, thus further testifying to the oxidation effect on particle surface.

For the sample treated at 773 K, the  $\zeta$ -pH curve is similar to that at 673 K, indicating that the oxidation is further intensified, as the variation in intensity and species of surface groups after heat treatment at 673 K is not so fierce.

### 3.3.3. Surface chemical analysis of DND-b powder

Table 1 compares the main elements (C, O and N) on the surface of the original DND-b powder and after the powder was treated at 773 K for 30 min, showing that oxygen had increased from 3.966% to 9.156%.

Fig. 5(A) shows the XPS survey spectra for the original sample (spectrum (a)) and the powder heated at 773 K for 30 min (spectrum (b)). A remarkable difference in the intensity of oxygen indicates the strong oxidation on the particle surface.

According to the C(1s) XPS spectrum for original DND-b (Fig. 5(B)), the binding energy peak is located at 284.8 eV, with a bulge on the higher binding energy side, indicating that the main chemical environment for carbon atom on DND-b are graphite and surface carbon structure with a  $sp^2$  hybridized C–H bonding, and that there are as well diamond structure and surface carbon structure with a  $sp^3$  hybridized C–H bonding. After thermal treatment, the bonding energy peak shifts from 284.8 to 286.8 eV, with an increase of 2 eV, that is, more carbon atoms might have been connected to oxygen-containing species, such as carbonyl, hydroxyl or nitro groups, or some oxygen-containing groups of a  $sp^3$  hybridized structure might have formed such as  $-\text{C}(\text{O})-\text{O}-$ ,  $=\text{C}=\text{O}$ ,  $\text{O}-\text{C}=\text{O}$ ,  $-\text{C}-\text{O}-\text{C}-$ ,  $-\text{C}(\text{H}_2)-\text{O}-\text{O}-\text{C}-$ . Nevertheless, there is still a shoulder

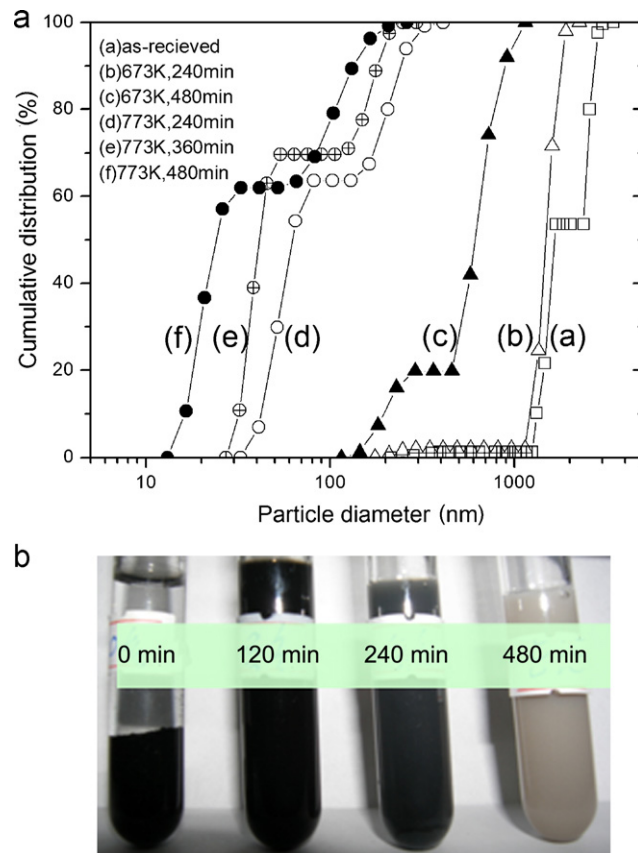


**Fig. 6.** Particle size distribution of powders before and after thermal treatments (top), and settlement of suspension of powders with and without thermal treatments at 773 K (bottom).

peak of binding energy at 284.6 eV, showing that there is still some  $sp^2$  hybridized carbon, which may be attributed to the residue of non-diamond carbon phase such as graphite after heat treatment at 773 K for 30 min.

In the O(1s) XPS spectra shown in Fig. 5(C), the binding energy peak shifts to 532.9 eV, with strengthened intensity, showing that large number of oxygen atoms have been adsorbed onto the DND-b surface and reacted with the surface atoms. In the N(1s) XPS spectra shown in Fig. 5(D), similar shift of N(1s) binding energy peak as that of C(1s) can be observed, indicating the oxidation effect of the amine groups. And, as a result, nitro groups, connected to carbon atoms on particle surface (C–N–O bonding), can be formed, as testified in corresponding change on FTIR spectra.

### 3.4. Dispersion property of particles

Samples heated under different thermal treatment conditions were dispersed in water. The pH value of the suspension was adjusted to 8–9, within which range, the absolute  $\zeta$ -potential of the particle is comparatively high and the dispersion is relatively stable. Cumulative size distribution curves of particles are shown in the top diagram of Fig. 6. Before thermal treatment, because of the low polarity of graphite on particle surface, DND-b shows poor dispersion behavior in aqueous medium, and the PSD is quite wide, as most of the particles are larger than  $1\ \mu\text{m}$  in diameter. With increasing temperature and treatment duration, the dispersion property of the powder improved, and the mean size of the aggregates declined significantly, with obvious increase of small particles. The asymptotic decline of particle size with increasing heating duration for 673 K (from curve (b) to (c)) and 773 K (from

curve (d) to (f)) shows that the heating time is a key parameter affecting particle dispersion. Compared to 673 K, samples treated at 773 K show better dispersion behavior. After heat treatment at 673 K for 240 min, the PSD curve is quite similar to that of the original one, and after treatment for 480 min, all particles can be reduced to less than 1  $\mu\text{m}$ . By comparison, samples treated at 773 K show smaller granularity, particularly the increase of smaller particles in the dispersed systems. According to the cumulative distribution curve, after 480 min of heating at 773 K, more than 60% of the dispersed particles are found to be smaller than 30 nm.

The bottom picture in Fig. 6 shows the suspension of powders after thermal oxidation at 773 K for different time durations. The powders were added into the aqueous media to prepare a suspension with a concentration of 1%, ultrasonicated for 30 min, and then laid to rest for 120 min. It can be seen from the photo that, with prolonging heating time from 0 to 480 min, the color of the suspensions turns from dark black (original sample) through black (sample heated for 120 min), and gray (sample heated for 240 min), to light gray (sample heated for 480 min), while the original powder settled totally. Evidently the dispersion behavior can be improved with the increase of heating time.

#### 4. Conclusions

The present study shows that, increase of surface oxygen-containing groups for DND can be accomplished by direct oxidation, and that increase of acidic polar groups can strengthen the electrostatic repulsion of particles, improve the hydrophilicity of particles, and provide more active anchoring points for the adsorption of surfactants, and improve the dispersion of particles.

At the initial stage of thermal oxidation, the main mechanism of graphite oxidation may be the rupture of C–C bonding in the graphite shell. An oxo-bridge (C–O–C) may form between adjacent carbon atoms, as shown by FTIR analysis. With intensification of oxidation, the oxo-bridge (C–O–C) can be broken, and due to effect of tension, the surface layer of carbon atoms would break from the inner layer to be stripped off, thus accelerating the removal of the graphite phase.

During thermal treatment, metal and metal compound may be exposed, which may react with the surrounding carbon atoms, hydroxyl or carbonyl groups to form metal oxide or carbonate. These impurities cannot be removed during thermal treatment, and calls for further purification.

#### Acknowledgements

This work was financially supported by Hunan Provincial Natural Science Foundation of China (Project No. 11JJ3054).

#### References

- Aleksenskii, A. E., Baidakova, M. V., Vul', A. Ya. & Siklitskii, V. I. (1999). The structure of diamond nanoclusters. *Physics of the Solid State*, 41, 668–671.
- Aleksenskii, A. E., Yagovkina, M. A. & Vul', A. Ya. (2004). Modification of surface and the physicochemical properties of nanodiamonds. *Physics of the Solid State*, 46, 685–686.
- Butenko, Yu. V., Kuznetsov, V. L., Chuvilin, A. L., Kolomiichuk, V. N., Stankus, S. V., Khairulin, R. A., et al. (2000). Kinetics of the graphitization of dispersed diamonds at "low" temperatures. *Journal of Applied Physics*, 88, 4380–4388.
- Cataldo, F. & Koscheev, A. P. (2003). A study on the action of ozone and on the thermal stability of nanodiamond. *Fullerenes, Nanotubes and Carbon Nanostructures*, 11(3), 201–218.
- Danilenko, V. V. (2004). On the history of the discovery of nanodiamond synthesis. *Physics of the Solid State*, 46(4), 595–599.
- Dolmatov, V. Yu. (2001). Detonation synthesis ultradispersed diamonds: Properties and applications. *Russian Chemical Reviews*, 70, 607–626.
- Dolmatov, V. Yu., Veretennikova, M. V., Marchukov, V. A. & Sushchev, V. G. (2004). Currently available methods of industrial nanodiamond synthesis. *Physics of the Solid State*, 46, 611–615.
- Gubarevich, T. M., Kostyukova, N. M., Sataeva, R. R. & Fomina, L. V. (1991). Study of the impurity composition of ultradisperse diamond. *Superhard materials*, 5, 31–34.
- Krüger, A., Kataoka, F., Ozawa, M., Fujino, T., Suzuki, Y., Aleksenskii, A. E., et al. (2005). Unusually tight aggregation in detonation nanodiamond: Identification and disintegration. *Carbon*, 43, 1722–1730.
- Kulakova, I. I. (2004). Surface chemistry of nanodiamonds. *Physics of the Solid State*, 46, 636–643.
- Kuznetsov, V. L., Aleksandrov, M. N., Zagoruiko, L. V., Chivilin, A. L., Moroz, E. M., Kolomiichuk, V. N., et al. (1991). Study of ultra disperse diamond obtained using explosion energy. *Carbon*, 29, 665–668.
- Kuznetsov, V. L., Chuvilin, A. L., Butenko, Yu. V., Mal'kov, I. Yu. & Titov, V. M. (1994). Onion-like carbon from ultra-disperse diamond. *Chemical Physics Letters*, 222, 343–348.
- Lyamkin, A. I., Petrov, E. A., Ershov, A. P., Sakovich, G. V., Staver, A. M. & Titov, V. M. (1988). Production of diamonds from explosives. *Doklady Akademii Nauk SSSR*, 302(3), 611–613.
- Mironova, E., Petrov, E. & Koretz, A. (2003). Chemical aspect of ultradispersed diamond formation. *Diamond and Related Materials*, 12, 1472–1476.
- Osswald, S., Yushin, G., Mochalin, V., Kucheyev, S. O. & Gogotsi, Y. (2006). Control of  $sp^2/sp^3$  carbon ratio and surface chemistry of nanodiamond powders by selective oxidation in air. *Journal of the American Chemical Society*, 128, 11635–11642.
- Sakovich, G. V., Komarov, V. F. & Petrov, E. A. (2002). Synthesis, properties, application, and production of nanometric diamonds. Part 1. Synthesis and properties. *Superhard materials*, 3, 1–15.
- Shenderova, O., Petrov, I., Walsh, J., Grichko, V., Grishko, V., Tyler, T., et al. (2006). Modification of detonation nanodiamonds by heat treatment in air. *Diamond and Related Materials*, 15, 1799–1803.
- Shenderova, O. A., Zhirnov, V. V. & Brenner, D. W. (2002). Carbon nanostructures. *Critical Reviews in Solid State and Materials Sciences*, 27, 227–356.
- Spitsyn, B. V., Davidson, J. L., Gradoboev, M. N., Galushko, T. B., Serebryakova, N. V., Karpukhina, T. A., et al. (2006). Inroad to modification of detonation nanodiamond. *Diamond and Related Materials*, 15(2/3), 296–299.
- Staver, A. M., Lyamkin, A. I., Gubareva, N. V. & Petrov, E. A. (1984). Ultradisperse diamond powders produced by explosion. *Fizika Goreniya i Vzryva*, 20(5), 100–103.
- Xu, K. & Xue, Q. J. (2007). Deaggregation of ultradispersed diamond from explosive detonation by a graphitization-oxidation method and by hydroiodic acid treatment. *Diamond and Related Materials*, 16, 277–282.
- Xu, X., Yu, Z., Zhu, Y. & Wang, B. (2005). Influence of surface modification adopting thermal treatments on dispersion of detonation nanodiamond. *Journal of Solid State Chemistry*, 178, 688–693.